p-i-n Diode Control Devices in *E*-Plane Technique

HEINRICH CALLSEN, MEMBER, IEEE, HOLGER H. MEINEL, SENIOR MEMBER, IEEE, AND WOLFGANG J. R. HOEFER, SENIOR MEMBER, IEEE

(*Invited Paper*)

Abstract—**The status of p-i-n diode control devices in *E*-plane technique, especially in integrated finline configurations, is reviewed. The circuit topologies, operating principles, and design considerations for state-of-the-art switches, attenuators, and digital modulators are discussed, and typical performance characteristics are presented. The superior performance of these components confirms that finline is the appropriate transmission medium for the realization of millimeter-wave p-i-n diode switches and attenuators in the low-power regime (up to some 10 W of CW power), where beam-lead p-i-n diodes can be used. By properly matching these devices to their finline embedding network, excellent broad-band characteristics can be achieved.**

I. Introduction

MILLIMETER-WAVE radio communication systems are highly attractive for spaceborne and terrestrial applications, both in civil and in military systems [1]–[3]. High antenna gain combined with small dimensions and broad bandwidth makes millimeter waves very advantageous for intersatellite communications, local area networks, and short-range mobile communications [4]–[6]. Such systems as well as multipurpose measurement equipment, surveillance receivers, and dual-frequency transceivers require broad-band control devices [7]–[10].

Section II of this paper deals with various shunt-type p-i-n diode switches and electronically variable attenuators. Single pole–single throw (SPST) switches with high isolation (up to 75 dB) and short switching time (as short as 0.5 ns) for switching and for analog amplitude modulation are presented, along with single pole–double throw (SPDT) and single pole–triple throw (SP3T) switches for multiple-way switching.

Section III is dedicated to a novel 180° digital phase shifter, which works as an analog amplitude modulator as well. Advanced millimeter-wave communication systems require high-speed 180° digital phase shifters with high carrier suppression. With such an RF modulator the transceiver can be made quite light, and the number of required millimeter-wave components can be reduced. High switching speed and broad bandwidth allow direct-sequence modulation and code multiplex operation for covert communications [11].

In Section IV, the circuit configuration and the operating principles of several other *E*-plane digital phase shifters will be reviewed. First, a biphase PSK modulator (180° phase shifter) for 29 GHz radio will be discussed. Then, several QPSK modulators using combinations of reflection-type p-i-n switches and 3 dB hybrids will be described, and their performance characteristics will be summarized.

Manuscript received January 25, 1988; revised July 28, 1988.

H. Callsen and H. Meinel are with the Radio and Radar Systems Group, AEG, Sedanstrasse 10, D-7900 Ulm, Federal Republic of Germany.

W. J. R. Hoefer is with the Laboratory for Electromagnetics and Microwaves, Department of Electrical Engineering, University of Ottawa, Ottawa, Ont., Canada K1N 6N5.

IEEE Log Number 8824994.

II. Broad-Band p-i-n Diode Switches and Attenuators

Finline is extremely well suited for realizing millimeter-wave p-i-n diode switches if power handling requirements permit the use of beam-lead p-i-n diodes. Finline has relatively low losses compared to other planar transmission lines; the transition to standard rectangular waveguide is a simple tapered slot, sometimes combined with a tapered dielectric protrusion for minimum return loss; and beam-lead semiconductor devices are easily implanted.

Among all millimeter-wave p-i-n diode switches, the shunt type with diodes mounted directly across the finline slot provides the largest bandwidth [12]. All other configurations such as series-type switches with p-i-n diodes placed across a series stub [13], [14] or shunt-type switch configurations with p-i-n diodes placed upon microstrip lines across the slot on the backside of the fins [15], [16] have only moderate bandwidth performance. Microstrip line p-i-n diode switches have potentially wide bandwidths as well, but due to the larger attenuation constant of microstrip these circuits have significantly higher losses [17].

A. Design of Shunt-Type p-i-n Diode Switches and Attenuators

Fig. 1 outlines the basic design of a shunt-type finline p-i-n diode switch. The mount is made in split-block

0018-9480/89/0200-0307$01.00

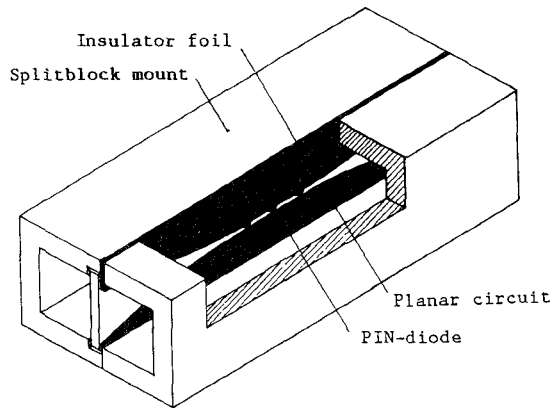

Fig. 1. Basic shunt-type finline p-i-n diode switch in finline.

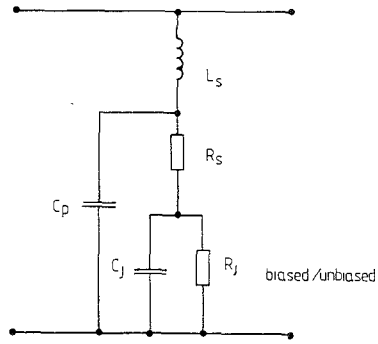

Fig. 2. Equivalent circuit of a beam-lead p-i-n diode

technique. The dielectric substrate with the printed circuit is suspended in the E plane of a rectangular waveguide with the help of two longitudinal slots. The substrate is made of a glass microfiber-reinforced PTFE material with a dielectric constant of 2.2 and a thickness of 254 μm or 127 μm. PTFE substrates such as RT/Duroid are admittedly the most appropriate materials for millimeter-wave finline circuits: their losses and their dielectric constants are very low, and they are robust and much easier to handle than hard substrate materials such as quartz. The metallic patterns are generated with standard photolithographic techniques. Several p-i-n diodes are placed across the finline slot to realize the switching function. For bias purposes, one of the fins is kept insulated from the metallic mount by means of a dielectric foil, for example a Mylar ribbon.

1) Embedding Network Analysis: The finline with an insulated fin is a complex waveguiding structure: in addition to the dominant finline mode it can sustain a parasitic quasi-TEM mode which is mainly concentrated in the insulating foil. If a p-i-n diode switch in such a structure is connected to a rectangular waveguide via a taper, most of the incident power is coupled to the finline mode and travels along the slot. However, a small fraction of the power is carried by the parasitic quasi-TEM mode in the dielectric foil inserted in the clamping region (see Fig. 1). In the ON state (reverse-biased diodes) the effect of the parasitic mode is negligible. However, in the OFF state, when the forward-biased diodes reflect the finline mode, the leakage due to the parasitic mode limits the maximum attainable isolation to about 40 dB. This may be acceptable for some applications, but if higher isolation is required the quasi-TEM mode must be suppressed by replacing the Mylar ribbon with a microwave resistive foil.

2) Equivalent Circuit of a p-i-n Diode: The equivalent circuit used to model the p-i-n diode is shown in Fig. 2. In principle, it is the circuit commonly used for millimeter-wave beam-lead p-i-n diodes. In our analysis, however, the series inductance L_s and the package capacitance C_p include the parasitics due to the embedding network. The capacitor C_j represents the junction capacitance of the p-i-n diode. The resistor R_s contains the bias-independent series resistance of the p-i-n diode, while the resistor R_j represents the junction resistance which depends on the bias current.

To obtain their equivalent circuit parameters in a finline environment, a number of single p-i-n diodes were mounted in typical switch configurations, and their transmission and return loss characteristics were measured over full waveguide bands. These data were then curve-fitted using SUPER-COMPACT, yielding the typical values given in Table I. It was found that in most p-i-n diodes the frequency-limiting parasitic element is a low junction resistance in the reverse-biased state.

3) Circuit Design and Optimization: The p-i-n diode switches are optimized for minimum insertion loss and maximum isolation over the maximum achievable bandwidth by optimizing diode spacings. The insertion loss is the most critical objective in p-i-n diode switch design, because it is very sensitive to the diode spacings. Therefore it must be optimized before all other considerations [18]. That set of diode spacings with minimum total length having minimum insertion and return loss has also the best isolation, and its characteristics depend least on frequency.

For switches with two or three diodes, the optimum diode spacings can easily be found with the Smith chart by determining the shortest electrical lengths required for impedance matching. Circuit analysis programs with optimizers are especially convenient when more than three diodes are involved.

4) Switching Considerations: The switching time of a p-i-n diode switch depends mostly on the selected p-i-n diode. For a given device it can be optimized via the waveform of the control signal. The critical phase in the switching process of shunt-type p-i-n diodes is the rise time —the time needed to switch from the forward-biased to the reverse-biased state. To minimize the rise time, the bias current must be made as low, and the reverse-bias voltage as high, as possible.

Mesa devices achieve switching times shorter than 1 ns. In comparison, planar p-i-n diodes are slow switches, with 50 ns at most. However, they have a higher reverse-bias resistance and a smaller junction capacitance than mesa devices; their figure of merit, as defined by Kawakami [19], is therefore higher than that of mesa diodes. Consequently, if high switching speed is essential, mesa devices

TABLE I
TYPICAL VALUES OF THE EQUIVALENT CIRCUIT ELEMENTS OF THREE COMMERCIAL BEAM-LEAD p-i-n DIODES MEASURED IN A FINLINE ENVIRONMENT

Diode Type	L_s [nH]	R_s [Ω]	C_p [fF]	C_j [fF]	$R_{j\,\text{for.b.}}$ [Ω]	$R_{j\,\text{rev.b.}}$ [Ω]
Alpha DSG 6474E	0.02	6	4	5	8	3220
Marconi DC 2602	0.07	5	12	6	5	3978
MA/COM 4P 800	0.06	3	12	16	3	3880

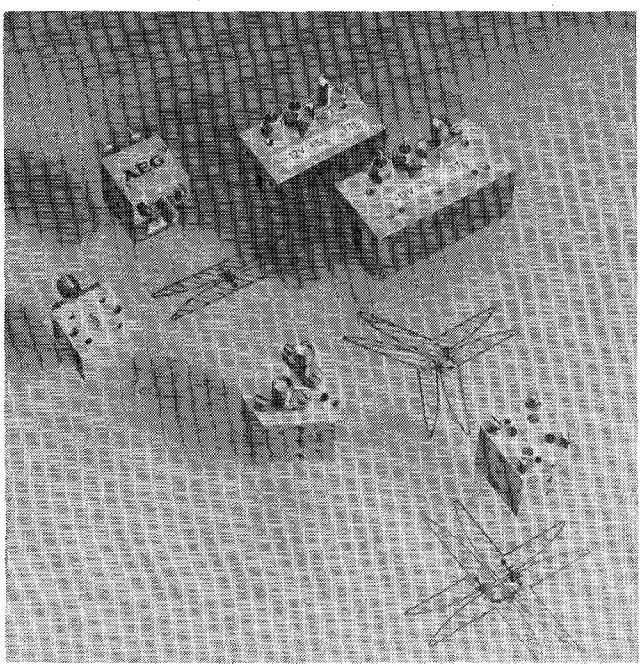

Fig. 3. p-i-n diode switches with integrated drivers for *K*-, *Ka*-, *V*-, and *T*-bands (courtesy of AEG, Ulm, Germany).

must be used, with a sacrifice in higher losses and narrower bandwidth. However, if the RF characteristics of the switch are more important, planar p-i-n diodes ought to be selected.

B. Measurements on Shunt-Type p-i-n Diode Switches

Fig. 3 shows p-i-n diode switches with integrated drivers for *W*-band, *Ka*-band, and *K*-band (top row, starting left). At the extreme left, a 150 GHz attenuator is displayed. Beneath, a *V*-band SPDT and a *V*-band SP3T switch are shown, together with their respective circuit layouts.

1) Single Pole–Single Throw Switches and Attenuators: SPST p-i-n diode switches were developed for frequencies between 18 and 150 GHz. Switches with high isolation were built for frequencies up to 100 GHz. The p-i-n diodes were selected according to switching time requirements and cost. A switch for *K*-band (18–26.5 GHz) featuring eight mesa p-i-n ND4028 diodes from Hewlett Packard was developed.

The achieved insertion loss is less than 1.6 dB, and the isolation is better than 75 dB over the entire waveguide band. Switching times are less than 2 ns.

A *Ka*-band p-i-n diode switch featuring six M/A-Com mesa p-i-n 4P800 diodes shows an insertion loss of less than 1.3 dB and an isolation of more than 70 dB over the

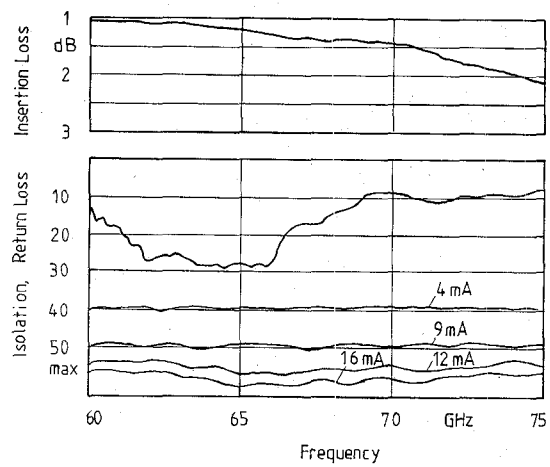

Fig. 4. Performance of a *V*-band p-i-n diode switch with four p-i-n DC 2602 diodes from Marconi.

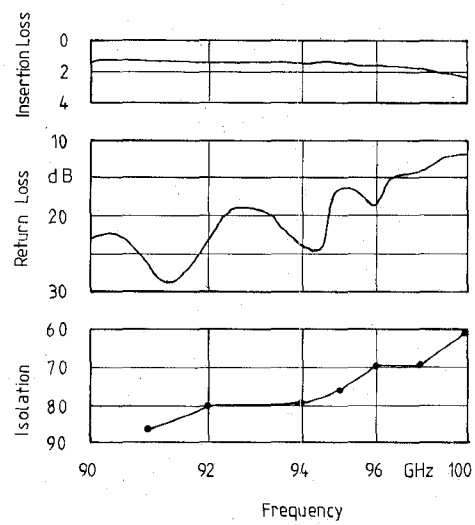

Fig. 5. Performance of a *W*-band p-i-n diode switch with six p-i-n DSG 6474E diodes from Alpha Industries.

entire *Ka*-band. The measured switching times are 35 ns (rise time) and 5 ns (fall time).

The swept frequency response of a four-diode attenuator for *V*-band operation (50–75 GHz) with mesa p-i-n DC-2602 diodes from Marconi is shown in Fig. 4. The attenuation may be varied from 2 dB to more than 50 dB. In the OFF state, the attenuation as a function of the forward bias current is nearly constant over the frequency. In the switch mode, the transfer time for both transitions is less than 1 ns. Fig. 5 shows the performance of a p-i-n diode switch with six diodes, designed for the 94 GHz range. In the ON state, the switch shows 1.8 dB of insertion loss and better

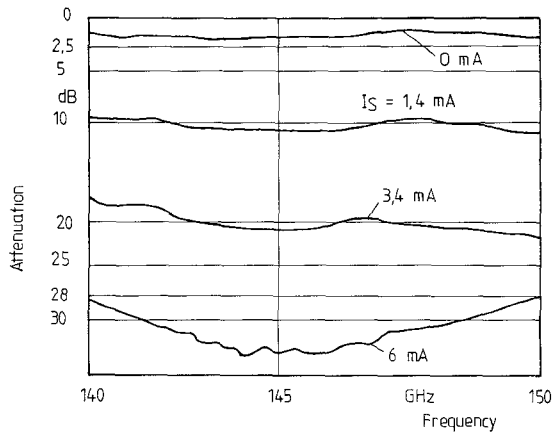

Fig. 6. Performance of a *T*-band p-i-n diode switch with three p-i-n DSG 6474E diodes from Alpha Industries.

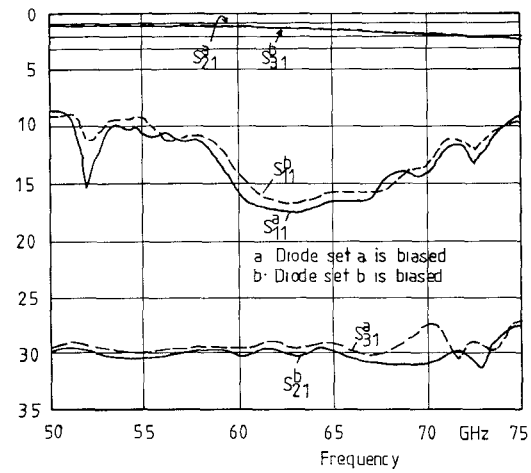

Fig. 7. Performance of a *V*-band SPDT p-i-n diode switch with two diodes in each output arm.

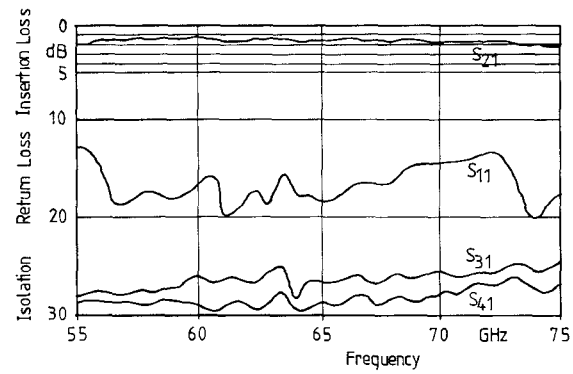

Fig. 8. Performance of a *V*-Band SP3T p-i-n diode switch with two diodes in each output arm.

than 15 dB of return loss. In the OFF state, both ports are isolated better than 70 dB. The measured rise and fall times are 150 and 15 ns, respectively. For operation in the 150 GHz range p-i-n switches were developed with up to three p-i-n diodes [20]. The insertion loss of a switch with three diodes (Fig. 6) is less than 2 dB, and the isolation amounts to more than 28 dB over the operating bandwidth between 140 GHz and 150 GHz. The achievable rise and fall times are less than 80 and 15 ns, respectively.

Beyer *et al.* [7], [8] developed a shunt-type finline attenuator for an automated *X*-band measurement system featuring three DSG 6474C beam-lead p-i-n diodes from Alpha Industries arranged as in Fig. 1. The insertion loss of this attenuator could be controlled between 0.5 and 20 dB over the entire *X*-band via the bias current. To obtain a frequency-independent attenuation, the bias current was automatically adjusted during a frequency sweep by a desktop computer through a digital interface. In this particular application exact control of the attenuation, rather than fast switching, was the primary design objective.

2) Single Pole–Double Throw p-i-n Diode Switches: If two p-i-n diode sets are placed across the slots in two arms of a finline Y or T junction, a single pole–double throw p-i-n diode switch is formed. The schematic finline layout is shown in the center of Fig. 3. Note that a set of two diodes about $\lambda/4$ apart is usually used instead of a single diode in each arm. To achieve maximum bandwidth, the first diode of each set must be placed as close as possible to the junction.

The finline T junction in standard rectangular waveguide has spurious resonances near the upper end of the available frequency range [21]. There are two ways to prevent the resonances:

1) The height of the surrounding rectangular waveguide can be reduced to shift the resonance frequency up, out of the band.
2) The electric field of the resonant mode can be short-circuited by a conducting wire across the junction near its center, running perpendicular to the substrate.

Several SPDT p-i-n diode switches with two diodes in each arm were developed for T/R switching in the 26.5–100 GHz range. Full waveguide bandwidth was achieved for frequencies up to 75 GHz. For higher frequencies, a 10 GHz bandwidth was obtained. The insertion loss of the SPDT switches is typically less than 2.5 dB, and the isolation is greater than 27 dB. The return loss is better than 10 dB, except at the band limits.

As switching speed was not important, planar p-i-n diodes (DSG 6474E) were used. Even though the switching times are shorter than 300 ns, they exceed those of SPST switches built with the same type of diodes. This is because SPDT devices must be biased very strongly to achieve the minimum insertion loss. The performance of a 50–75 GHz SPDT p-i-n diode switch is shown in Fig. 7.

3) Single Pole–Triple Throw p-i-n Diode Switches: By analogy to the SPDT switch, an SP3T p-i-n diode switch is formed with a finline cross-junction. Diode sets are mounted in three arms of the cross-junction. A schematic layout of the SP3T p-i-n diode switch is shown at the bottom of Fig. 3. Again, a set of two diodes instead of a single diode is usually placed in each arm. All fins must be kept insulated from the mount. A control signal is fed via four soldering pins to the diodes such that two sets of p-i-n diodes are forward biased while the third set is reverse

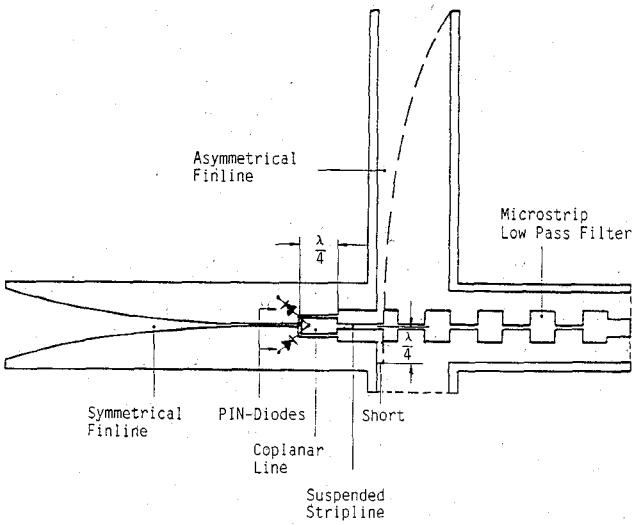

Fig. 9. Basic planar circuit of the PSK/ASK modulator.

biased (Fig. 3, bottom right). An SP3T p-i-n diode switch was developed for the 60 GHz range. The characteristics of this switch are shown in Fig. 8. The insertion loss is less than 2.5 dB in the measured frequency range. The isolation amounts to more than 25 dB. This switch was developed with sets of two diodes in each arm, because this amount of isolation was sufficient. If system specifications require higher isolation, the number of p-i-n diodes in each arm can be increased.

III. 180° p-i-n Diode Digital Phase Shifter

The basic planar finline circuit of a 180° digital phase shifter is similar to that of millimeter-wave balanced finline mixers [22], but instead of Schottky diodes p-i-n diodes are implemented.

A. Circuit Description

The basic circuit of the phase shifter is shown in Fig. 9. It consists of the following four subcircuits:

a) a p-i-n diode switchable balanced/unbalanced transformer, consisting of a coplanar line interfaced with a finline and suspended stripline, and a pair of p-i-n diodes;
b) a tapered transition between the waveguide input port and the finline port of this balun;
c) a transition between the suspended stripline port of this balun and the waveguide output;
d) a low-pass filter linking the p-i-n diodes with the control signal port.

The switchable balun is the actual phase shifter circuit. The transitions connect the phase shifter with the waveguide system, while the low-pass filter links the p-i-n diodes to the control signal.

The balun is formed by a $\lambda/4$ coplanar line with standard rectangular waveguide cross section. One end is connected to the finline, while the other is connected to the suspended stripline which has a reduced cross section to

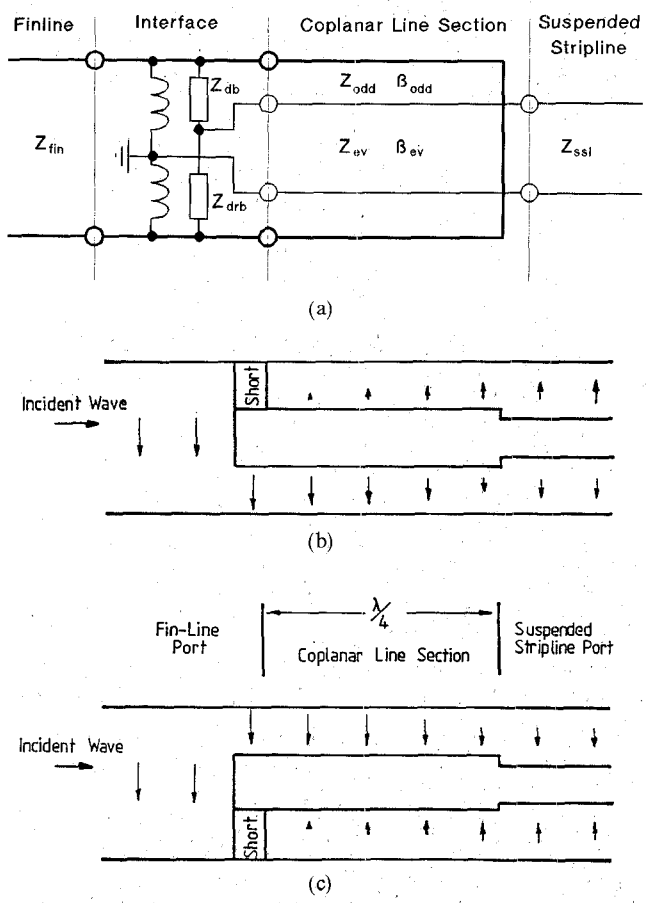

Fig. 10. Principle of operation of a switchable balun. (a) Equivalent circuit. (b) and (c) Field orientation in the two switching states. (Arrows indicate the direction and intensity of the electric field.)

suppress higher order mode propagation [22]. The p-i-n diodes are mounted across the coplanar line at the interface with the finline, antiparallel to the center conductor, as shown in Fig. 9. The coplanar line with standard waveguide cross section sustains two propagating modes: the even mode, a quasi-TEM mode resembling the dominant mode in suspended stripline, and the odd mode, a waveguide mode similar to the dominant finline mode. The even mode links the coplanar line with the suspended stripline, while the odd mode links it with the finline.

To activate the balun function, a control signal is applied. As the two diodes are connected in antiparallel, one of them is forward biased, whereas the other is reverse biased. The short-circuited p-i-n diode connects the center conductor of the coplanar line to one of the outer conductors. Hence, an incoming wave is split into an even and an odd mode with equal amplitudes. As a result, mode conversion takes place, and the finline input is coupled to the suspended stripline output.

This situation is described by the equivalent circuit in Fig. 10(a), from which the following relations between the line impedances can be obtained:

$$Z_{\text{fin}} = \frac{4Z_{\text{ev}}^2}{Z_{\text{ssl}}} \quad \text{if} \quad Z_{\text{ssl}} = Z_{\text{asfin}},$$

$$Z_{\text{db}} \ll Z_{\text{ev}}, \quad \text{and} \quad Z_{\text{drb}} \gg Z_{\text{ev}} \qquad (1)$$

where

Z_{fin} = impedance of the symmetrical finline
Z_{ev} = even-mode impedance of the coplanar line
Z_{ssl} = impedance of the suspended stripline
Z_{asfin} = impedance of the asymmetrical finline
Z_{db} = impedance of the biased diode
Z_{drb} = impedance of the reverse-biased diode.

In this formula, parasitics due to discontinuities have been neglected, and the impedance of the reverse-biased diode has been considered negligible vis-à-vis the finline impedances. A wave incident on the finline is phase shifted by 180°; i.e., the orientation of the electric field in the coplanar line is switched when the position of the short is exchanged as shown in Fig. 10(b) and (c). This 180° phase shift is independent of frequency, in spite of changes in characteristics due to frequency-dependent elements of the actual circuit. If the shorts in Fig. 10(b) and (c) are removed, or if the diodes are unbiased, a wave incident from the finline port excites only the odd mode, which is short-circuited and reflected by the reduced waveguide cross section of the suspended stripline. A wave incident at the stripline port excites the even mode only, which is open-circuited at the interface with the finline. If the diodes are unbiased, no mode conversion occurs. The degree of isolation between input and output port in this state depends on the symmetry of the circuit. Thus, amplitude modulation can be performed by varying the bias current with a unipolar modulating signal. The transition between the suspended stripline and the asymmetrical finline is similar to normal probe-type transitions between waveguide and coaxial line. The center conductor of the stripline is connected to the asymmetrical fin via the low input impedance of the microstrip low-pass filter. The asymmetrical finline is short-circuited at a quarter wavelength beyond the junction (strip) to maximize magnetic coupling.

The mount is made in split-block technique. The planar circuit is fabricated on a 254-μm-thick RT-Duroid 5880, a fiberglass-reinforced PTFE with a relative dielectric constant of 2.2.

B. Experimental Results

The measured results are depicted in Figs. 11 and 12. The phase shift between the two states is given in Fig. 11. In the measured frequency range from 30 GHz to 40 GHz (the operating range of the network analyzer) the phase shift increases continuously from 181° to 183°. The ripple in the measured phase difference is due to the measurement equipment.

As Fig. 12 reveals, the measured amplitude imbalance is less than 0.1 dB in the entire *Ka*-band. The insertion loss is less than 1.3 dB in the frequency range from 28 GHz to 37 GHz and less than 1.7 dB in the entire *Ka*-band. Finally, the return loss for the two PSK states is better than 11 dB in the entire *Ka*-band, and better than 15 dB between 30 GHz and 40 GHz. It is only slightly different in the two states.

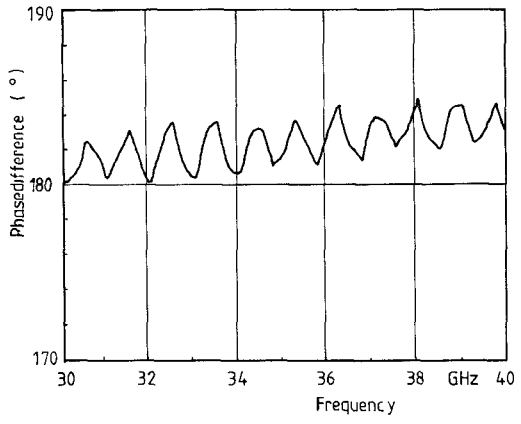

Fig. 11. Measured phase difference between the two states of the PSK modulator shown in Fig. 9.

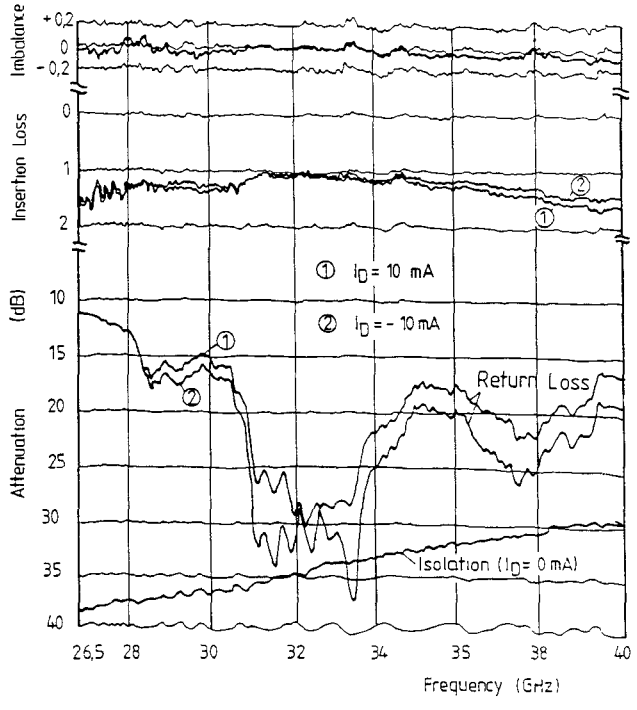

Fig. 12. The measured amplitude imbalance, insertion loss, and return loss for the two states during PSK modulation, and maximum isolation for unbiased diodes of the modulator in Fig. 9.

The isolation between the input and the output port for unbiased diodes decreases continuously from 38 dB at 26.5 GHz to 29 dB at 40 GHz; in the same way the ASK modulation depth decreases from 36.5 dB at 26.5 GHz to 27.5 dB at 40 GHz.

These results were obtained from a modulator developed with high-speed mesa p-i-n diodes (DC 2602 from Marconi). Hence, the modulator can be operated with modulation frequencies up to several hundred MHz.

IV. Alternative *E*-Plane Digital Modulators

A. Transmission-Type BPSK Modulator

Another 180° phase shifter which exploits the principle of transmission path switching has been reported by Thorpe

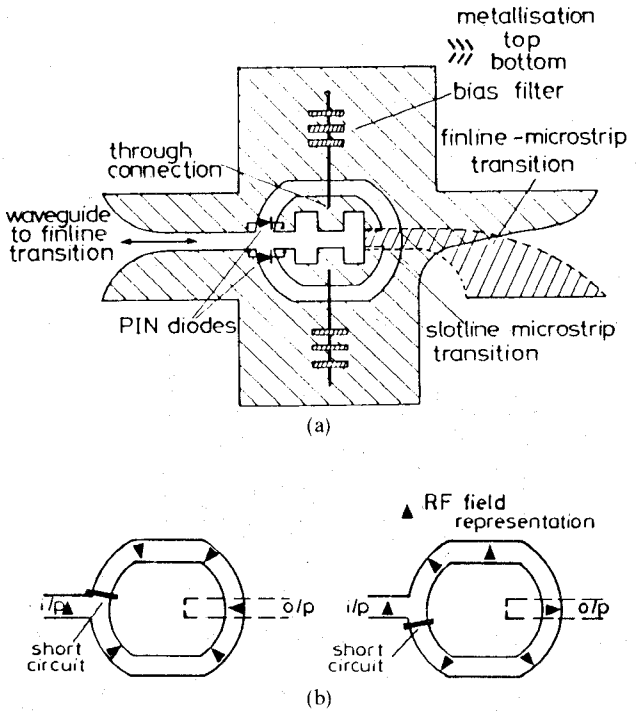

Fig. 13. BPSK-modulator by Thorpe [23], [24]. (a) Circuit layout. (b) Principle of operation.

[23], [24]. It has been developed for use in 29 GHz radio distribution systems.

1) Circuit Description and Operation: The layout of the BPSK modulator is shown in Fig. 13(a). The carrier enters the modulator through a waveguide-to-finline taper. The transmission path is then split into the slotlines forming a ring which, at the far end, is magnetically coupled to a microstrip on the back of the substrate. Finally, an antipodal microstrip-to-waveguide transition leads to the output port. The beam-lead diodes are bonded across the arms of the T junction and can be biased separately to achieve fast switching times. To this end, the central island is split by a double-ended slotline quarter-wave transformer which ensures good RF continuity while separating the modulating signals applied to the diodes.

The principle of circuit operation is visualized in Fig. 13(b). The two possible bias states are shown side by side, the forward-biased diode being approximated by a short circuit, and the reversed-biased diode by an open circuit. The arrows indicate the polarity of the electric field in the slot and show how the bias change produces a 180° phase shift at the output port.

Even though the phase shift is essentially independent of the frequency—it is affected only by the diode parasitics—the total insertion loss of the modulator varies slightly with frequency due to the standing wave pattern forming in the ring.

2) Performance Characteristics: The modulator was able to switch at least 150 mW of power in the 27.5 to 29.5 GHz band without any noticeable change in performance. Less than 3 dB insertion loss was measured over that range. Isolation between input and output ports was greater

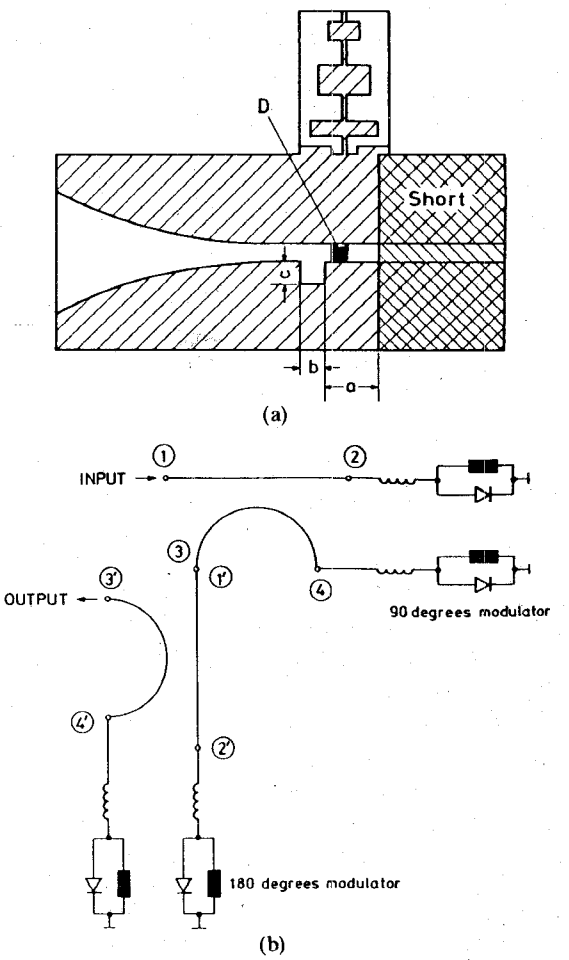

Fig. 14. QPSK modulator by Kpodzo *et al.* [25]. (a) Slot pattern of reflection-type phase modulator with HPND-4050 p-i-n diodes from Hewlett Packard. WR-62 enclosure. Substrate: 0.254 mm thick, $\epsilon_r = 2.22$.

180° phase shift: $a = 3.85$ mm, $b = 0.2$ mm, $c = 1.0$ mm
90° phase shift: $a = 2.90$ mm, $b = 0.2$ mm, $c = 1.5$ mm

(b) Equivalent circuit of the QPSK modulator.

than 25 dB. Amplitude imbalance between the two states was less than 1 dB, and phase imbalance less than 3°. A 100 Mbit/s data rate was achieved.

Just like the modulator described in Section III, Thorpe's circuit can also be used for ASK modulation. To this end, one of the diodes is kept permanently reverse biased, while the other is switched on and off at the desired modulation rate. An on–off ratio greater than 25 dB has been measured over the 27.5 to 29.5 GHz range for this mode of operation.

B. Reflection-Type PSK Modulators

In this type of modulator, a short-circuited length of transmission line is switched on and off with a p-i-n diode. The phase difference between reflections in the two states depends on the electrical length of the switched line. Either a circulator or a 3 dB hybrid is used to separate the incident from the reflected wave.

Due to the frequency dependence of the electrical length of the switched line, reflection-type modulators are inherently narrow-band devices. The presence of diode para-

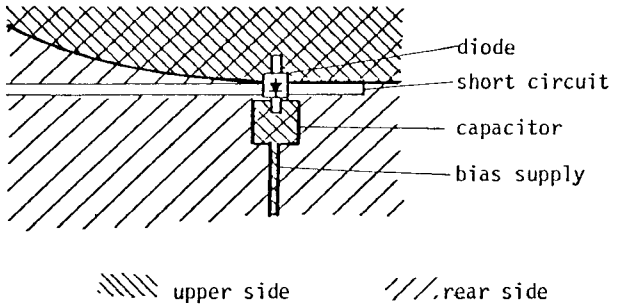

Fig. 15. Slot pattern of reflection-type phase modulator with series capacitor for broad-band performance (from Schieblich, Goebel, and Beres [26]).

sitics compounds this disadvantage. The design of such a modulator amounts to creating a matching network which transforms the complex impedances of the diode in the ON and the OFF state into reflection coefficients which have a constant phase difference over the desired bandwidth.

1) Typical Circuit Realizations: *E*-plane reflection-type phase modulators have been described by Kpodzo *et al.* [25], Schieblich *et al.* [26], and Gajda and Verver [27].

The layout of the phase shifter employed in [25] is shown in Fig. 14(a). The matching network consists of a short-circuited finline section and an inductive notch in the lower fin. The circuit is suspended in a WR-62 waveguide housing. The dimensions yielding both a 90° and a 180° phase shifter for 15 GHz operation are given. Fig. 14(b) shows how a quadriphase (QPSK) modulator can be realized by cascading two 3 dB hybrids whose ports 2 and 4 are both terminated either in 180° or 90° phase modulators.

In order to increase the bandwidth of reflection-type phase shifters, Schieblich *et al.* [26] propose to add a capacitance in series with the p-i-n diode, thus obtaining a bandwidth larger than 25 percent for a $\pm 2°$ prescribed phase difference. The realization of this principle is shown in Fig. 15. Note that the diode, the series capacitor, and the bias circuitry are all mounted on one side of the substrate, while the finline RF circuit is realized on the other side.

Finally, Fig. 16 shows a QPSK modulator of the type realized by Gajda and Verver [27]. Unlike the series configuration by Kpodzo *et al.*, it consists of a parallel combination of two 180° biphase modulators, fed by a 3 dB quadrature hybrid. The output signals of the phase shifters are merged in an in-phase combiner to produce the QPSK signal (Fig. 16(a)). The parallel combination has a much higher insertion loss than the series arrangement due to the additional loss in the input hybrid and the output combiner; however, it allows the biphase modulators to function as linear amplitude modulators. Fig. 16(b) shows the layout of the complete integrated QPSK modulator. (The metallization is white, the substrate is black.) Along the main diagonal one can distinguish two 3 dB hybrids with their outer ports terminated in reflection-type phase shifters. The input hybrid and the output combiner are also clearly visible.

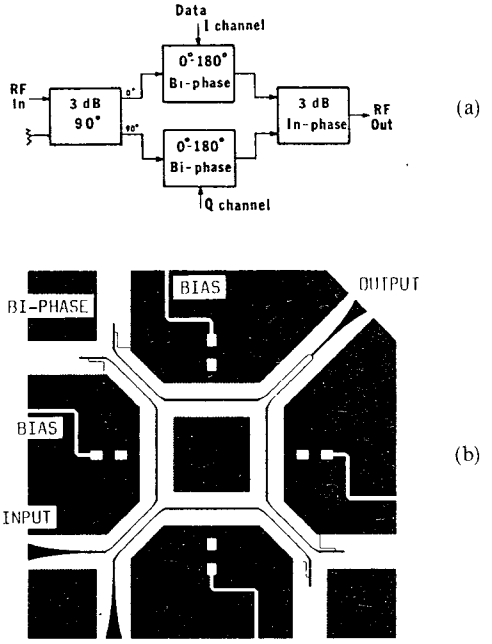

Fig. 16. Parallel-type QPSK modulator by Gajda and Verver [27]. (a) Schematic configuration. (b) Circuit layout of the integrated modulator.

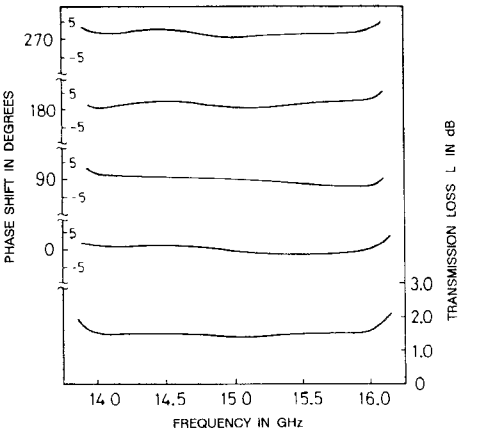

Fig. 17. Insertion loss and phase shift of the series-type QPSK modulator in Fig. 14(b) (from Kpodzo *et al* [25]).

2) Performance Characteristics: The series-type QPSK modulator by Kpodzo *et al.* [25] was realized in two versions, one in a WR-62 enclosure designed for 15 GHz, the other in a WR-28 enclosure for 30 GHz. The first had an insertion loss of 1.7 dB at 15 GHz, while the second had 2.2 dB at 30 GHz. Both versions had a bandwidth of 15 percent, over which the phase shift remained constant within 5°. A switching time of 2 ns for the HPND-4050 diodes (Hewlett Packard) has been obtained. Fig. 17 shows the transmission loss and the phase shift of the modulator for 15 GHz over a 2 GHz bandwidth.

Fig. 18 demonstrates the increase in bandwidth achieved by Schieblich *et al.* [26] by connecting a capacitor in series with the p-i-n diode. The phase shift remains constant within $\pm 2°$ over a bandwidth of 25 percent, and the amplitude imbalance is less than 1 dB. Since typical *E*-plane hybrids have a similar bandwidth, QPSK modulators

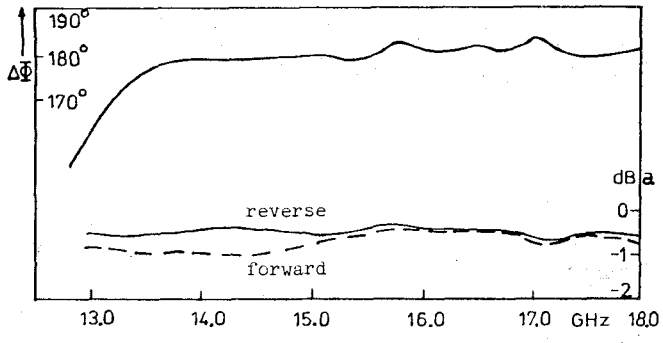

Fig. 18. Insertion loss and phase shift of the broad-band phase shifter in Fig. 15 (from Schieblich *et al.* [26]).

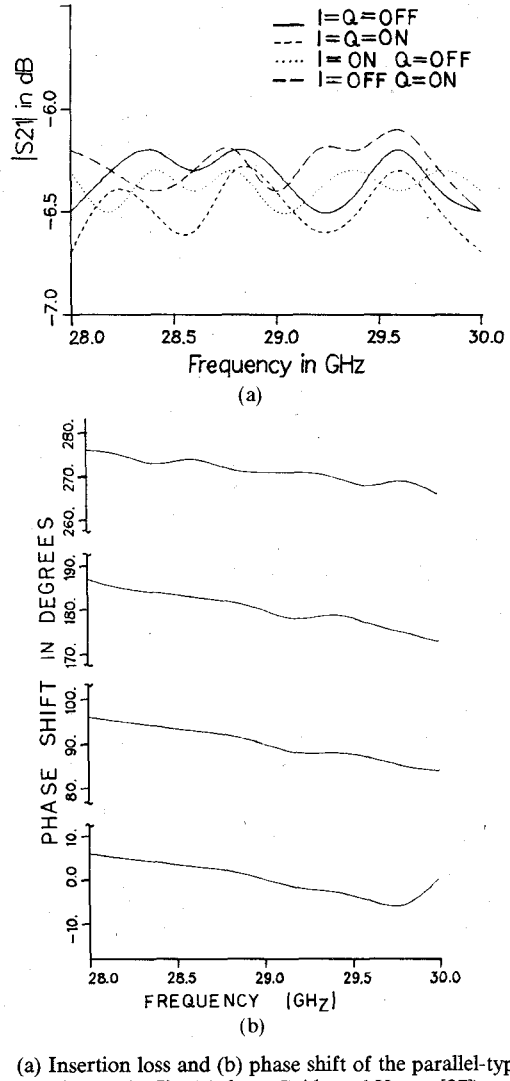

Fig. 19. (a) Insertion loss and (b) phase shift of the parallel-type QPSK modulator in Fig. 16 (from Gajda and Verver [27]).

could be realized with 25 percent bandwidth by employing capacitively loaded reflection-type switches.

The parallel-configured QPSK modulator by Gajda and Verver [27] was realized on 254-μm-thick RT/Duroid in a WR-28 enclosure for operation at 28.4 GHz. From 28 to 30 GHz, the insertion loss was around 6.5 dB, with a 0.5 dB amplitude unbalance and a 5° phase error. The latter could probably be improved by the broad-banding techniques mentioned above. Four beam-lead Alpha DSG6474 p-i-n diodes were used. Fig. 19 shows the performance of the modulator over a 2 GHz bandwidth. The high insertion losses occur essentially in the input hybrid and the output combiner. Each of the two biphase modulators consisting of one 3 dB hybrid and two phase shifters has an insertion loss of 1.5 dB. Insertion loss was sacrificed for the ability to use the module as an amplitude modulator. Data rates of 2.7 Mbit/s have been achieved.

V. Conclusion

The status of p-i-n diode control devices in *E*-plane technique, especially in integrated finline configurations, has been reviewed. Switches, attenuators, and digital modulators with state-of-the-art performance have been described. Circuit configurations and operating principles were explained, and important design principles were discussed.

The superior performance of these components confirms that finline is the appropriate transmission medium for the realization of millimeter-wave p-i-n diode switches and attenuators in the low-power regime (up to some 10 W of CW power), where beam-lead p-i-n diode devices can be used. By properly matching these devices to their finline embedding network, excellent broad-band characteristics can be achieved.

References

[1] J. R. Forrest, "Terrestrial mobile communications—Cellular, satellite and their interfaces," in *Proc. 15th European Microwave Conf.*, Sept. 1985, pp. 38–47.

[2] A. Blaisdell and F. G. Loso, "Integrated frontend designed for multichannel EHF radios," *Microwave Syst. News*, pp. 118–127, Apr. 1987.

[3] J. B. Schultz, "Milstar progresses despite high cost and technology risks," *Defense Electronics*, pp. 92–98, June 1984.

[4] W. Menzel and W. Herzig, "MM-wave technology for satellite communications" (in German), *Telematica '86*, vol. 3, pp. 211–224, 1986.

[5] H. Meinel, "A Survey of terrestrial mm-wave radio systems for commercial users," in *MELECON'87 Dig.* (Rome, Italy), Mar. 1987, pp. 115–120.

[6] H. J. Thomas, G. L. Siqueira, and R. S. Cole, "MM-wavelength cellular radio: Propagation measurements 55 GHz," in *Proc. 16th European Microwave Conf.* (Dublin), Sept. 1986, pp. 221–226.

[7] A. Beyer, W. Mueller-Gronau, and I. Wolff, "A computer-controlled integrated microwave measurement system in finline technique for automatic material parameter measurements," in *1984 IEEE MTT-S Symp. Dig.* (San Francisco), 1984, pp. 345–347.

[8] A. Beyer, W. Mueller-Gronau, and I. Wolff, "A method for measuring the complex magnetic and dielectric material parameters of microwave ferrites," in *Proc. 14th European Microwave Conf.* (Liège, Belgium), Sept. 1984, pp. 213–218.

[9] W. Stahl, E. Fliege, H. Dreizler, and R. Schwarz, "A microwave Fourier transform spectrometer for lower *K*-band," *Z. Naturforsch.*, vol. 39a, pp. 354–356, 1984.

[10] A. G. Cardiasmenos, "Future trends in mm-wave receiver design," *Military Electronics/Countermeasures*, pp. 49–56, June 1981.

[11] W. Koerner and W. Menzel, "Low probability of intercept in communication networks using mm-waves," *Military Technology*, pp. 201–206, June 1985.

[12] B. Adelseck, H. Callsen, H. Meinel, W. Menzel, and K. Solbach, "A survey of planar integrated mm-wave components," *Radio Electron. Eng.*, vol. 52, no. 1, pp. 46–50, Jan. 1982.

[13] W. Menzel and H. Callsen, "Integrated finline components and subsystems at 60 and 94 GHz," *IEEE Trans. Microwave Theory Tech.*, vol. MTT-31, pp. 142–146, Feb. 1983.

[14] H. El Hennawy and K. Schuenemann, "Computer-aided-design of finline detectors, modulators and switches," *Arch. Elek. Übertragung.*, vol. 36, pp. 49–56, Feb. 1982.
[15] H. Meinel and B. Rembold, "New millimeter-wave finline attenuators and switches," in *1979 IEEE MTT-S Symp. Dig.* (Orlando, FL), 1979, pp. 249–252.
[16] R. B. Greed, "Integrated microstrip and antipodal finline leads to enhanced PIN diode components," in *Proc. 14th European Microwave Conf.* (Liège, Belgium), 1984, pp. 593–597.
[17] R. S. Tahim, T. Pham, and K. Chang, "*W*-band integrated circuit PIN switches," *Microwave J.*, pp. 133–138, Dec. 1986.
[18] R. V. Garver, *Microwave Diode Control Devices*. Dedham, MA: Artech House, ch. 6.
[19] S. Kawakami, "Figure of merit associated with variable-parameter one-port for RF switching and modulation," *IEEE Trans. Circuit Theory*, vol. CT-12, no. 3, pp. 321–328, Sept. 1965.
[20] H. Callsen, "Finline PIN-diode attenuator and switch for the 140 GHz range," in *8th Int. IR & MM-Wave Conf. Dig.*, Dec. 1983, F3.4/1-2.
[21] K. Solbach, H. Callsen, and W. Menzel, "Spurious resonances in asymmetrical finline junctions," *IEEE Trans. Microwave Theory Tech.*, vol. MTT-29, pp. 1193–1195, Nov. 1981.
[22] W. Menzel and H. Callsen, "Ultrabroadband balanced finline mixer," *Electron. Lett.*, vol. 18, no. 17, pp. 724–725, 19th Aug. 1982.
[23] W. Thorpe, "An *E*-plane broadband bi-phase balanced modulator for *Ka*-band," in *1983 IEEE MTT-S Int. Microwave Symp. Dig.*, (Boston, MA), pp. 513–515.
[24] W. Thorpe and J. D. Gilliland, "29 GHz *E*-plane biphase modulator," *Electron. Lett.*, vol. 19, no. 3, pp. 107–109, Feb. 1983.
[25] E. Kpodzo, K. Schuenemann, and G. Begemann, "A quadriphase fin-line modulator," *IEEE Trans. Microwave Theory Tech.*, vol. MTT-28, pp. 747–752, July 1980.
[26] C. Schieblich, U. Goebel, and V. Beres, "Broadband reflection-type phase modulators," in *1983 IEEE MTT-S Int. Microwave Symp. Dig.* (Boston, MA), pp. 510–512.
[27] G. B. Gajda and C. J. Verver, "Millimeter-wave QPSK modulator in fin line," in *1986 IEEE MTT-S Int. Microwave Symp. Dig.* (Baltimore, MD), pp. 233–236.

✠

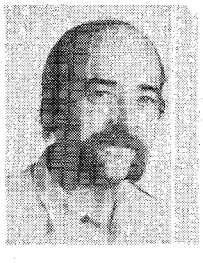

Heinrich J. Callsen (M'84) was born in Söby, Schleswig-Holstein, Federal Republic of Germany (FRG), on April 6, 1948. He received the Ing.-grad. degree from the Staatliche Ingenieurschule Lübeck, FRG, in 1971 and the Dipl.-Ing. degree from the Technische Universität Berlin in 1978.

He joined the New Technologies Department of AEG in Ulm, FRG, working on mm-wave *E*-plane integrated circuits and standard waveguide components. His special interests are detectors, balanced mixers, p-i-n diode switches, phase shifters, and directional couplers. Since 1987 he has been a systems engineer in the Radio and Radar Systems Division of AEG in Ulm.

✠

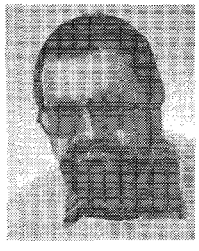

Holger Meinel (SM'84) is Manager of the RF-Systems Department in the Radar Division of AEG-Telefunken, responsible for the development of ECM and radar systems up to the millimeter-wave range. He was Supervisor of the radar subsystems group and of the millimeter-wave integration group, responsible for the development of hybrid technology for millimeter-wave radar and communication systems with emphasis on commercial and scientific applications. As a Research and Development Engineer in the Advanced Technology Department of AEG-Telefunken, he has designed components for a 35 GHz anticollision radar for cars. He is the author or coauthor of more than 50 technical papers and holds seven patents.

✠

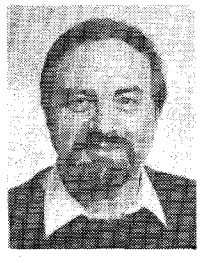

Wolfgang J. R. Hoefer (M'71–SM'78) received the diploma in electrical engineering from the Technische Hochschule Aachen, Aachen, Germany, in 1964, and the D. Ing. degree from the University of Grenoble, Grenoble, France, in 1968.

After one year of teaching and research at the Institute Universitaire de Technologie, Grenoble, France, he joined the Department of Electrical Engineering, University of Ottawa, Ottawa, Ont., Canada, where he is currently a Professor. His sabbatical activities have included six months with the Space Division of the AEG-Telefunken in Backnang, Germany, six months with the Electromagnetics Laboratory of the Institut National Polytechnique de Grenoble, France, and one year with the Space Electronics Directorate of the Communications Research Centre in Ottawa, Canada. His research interests include microwave measurement techniques, millimeter-wave circuit design, and numercial techniques for solving electromagnetic problems.

Dr. Hoefer is a registered Professional Engineer in the province of Ontario, Canada.